Journal of Applied Physics ARTICLE scitation.org/journal/jap

A comprehensive theoretical picture of E centers in silicon: From optical properties to vacancy-mediated dopant diffusion

Cite as: J. Appl. Phys. **127**, 085703 (2020); doi: 10.1063/1.5140724
Submitted: 30 November 2019 · Accepted: 7 February 2020 ·
Published Online: 24 February 2020

G. Herrero-Saboya,[1,2,a)] L. Martin-Samos,[3] A. Jay,[2] A. Hemeryck,[2] and N. Richard[1]

AFFILIATIONS

[1]CEA, DAM, DIF, F-91297 Arpajon, France
[2]LAAS-CNRS, Université de Toulouse, CNRS, Toulouse, France
[3]CNR-IOM/Democritos National Simulation Center, Istituto Officina dei Materiali, c/o SISSA, via Bonomea 265, IT-34136 Trieste, Italy

Note: This paper is part of the Special Topic on Defects in Semiconductors 2020.
[a)]**Author to whom correspondence should be addressed:** gherrero@laas.fr

ABSTRACT

Among the common vacancy-related point defects in silicon, the E center is one of the most prominent due to its degrading effect in silicon-based technology. Even though it has been the subject of extensive experimental and theoretical studies, a comprehensive theoretical model capable of reproducing the experimental evidence for all three dopants (P, As, and Sb) is still missing. Guided by a Jahn-Teller model, we are able to reproduce the absorption bands and the transition probability between equivalent geometries of the defect at low temperatures by including many-body-perturbation corrections based on the GW approximation on top of the density functional theory. At higher temperatures, vacancies become mobile centers, enabling the reorientation of the whole defect and contributing to the dopant diffusion. The underlying mechanisms of the vacancy-mediated dopant diffusion are revisited, characterizing the activation energies of such technologically relevant processes and obtaining quantitative results in good agreement with experiment.

I. INTRODUCTION

One of the most abundant point-like defects in n-type doped silicon is the E center. It consists of a silicon vacancy trapped next to a donor element (most commonly P, As, and Sb). Besides their known electronic activity,[1] E centers can play important roles in specific performance losses and long term degradation processes. The phosphorous–vacancy complex (also denoted as the PV center) is postulated, for instance, to be at the origin of the two level dark current-random telegraph signal[2–5] in image sensors, since the defect reorientation at room temperature is believed to cause the variation of the measured conductivity. The arsenic-vacancy (AsV) and antimony–vacancy (SbV) complexes are considered crucial in dopant diffusion as the vacancy-mediated contribution seems to be comparable to or even higher than the interstitial-mediated mechanism.[6] The possibility for a center to exhibit and/or participate in the aforementioned phenomena relies strictly on the details of its potential energy surface (PES) and the underlying reaction mechanisms that could be activated.

E centers were first characterized by Watkins and Corbett during a series of Electronic Paramagnetic Resonance (EPR) studies on point defects in silicon.[7,8] They reported that the ground state configuration of the neutral E center presents a *pairing* geometry: one of the three interatomic distances between the three silicon atoms adjacent to the vacancy is shorter than the other two; see Fig. 1. Moreover, in Refs. 7 and 8, two temperature regimes were distinguished. At low temperature, stress measurements revealed the existence of *three degenerate ground state geometries* [P_1, P_2, and P_3 in Fig. 1(b)] separated by an *energy barrier* of 60–70 meV. Later optical absorption studies[9] of PV^-, AsV^-, and SbV^- showed a ground state Jahn-Teller distortion of an opposite sign. In this configuration, known as *resonant*, one of the silicon bonds is longer than the other two (see Fig. 1). The change of Jahn–Teller distortion

with the charge state, together with the presence of degenerate ground states, was explained by a simple single-electron orbital model,[10] according to which the PES is predicted to exhibit the form of a *Mexican hat*. Furthermore, Watkins hypothesized[10] that the *energy barrier* between equivalent minima for the neutral systems actually corresponds to the energy difference between pairing and resonant configurations. At higher temperatures, energy barriers of 0.90 up to 1.30 eV for P, As, and Sb were observed. Such barriers were assigned to the *reorientation of the vacancy–dopant axis*, i.e., the reorientation of the whole vacancy–dopant complex. It was also postulated that this reorientation process, followed by a *dopant–vacancy exchange*, would characterize the vacancy-mediated dopant diffusion.

On the modelling side, the energy ranking of these configurations is not consistent between different studies:[11–16] the ground state geometry for the PV center was found to be a pairing configuration for both neutral and negative charge states in Ref. 11 (see also Ref. 12 for the neutral charge state) but a resonant one in Ref. 13. Later studies reported a rather flat PES with multiple *metastable* minima, comprising pairing, resonant, and, in some cases, breathing ($\mathcal{B}$) configurations.[14,15] Only for the AsV center has the measured Jahn–Teller distortion at neutral and negative charge states (pairing and resonant distortions, respectively) been correctly reproduced.[16] In all the aforementioned works, the assessment for metastability has only been based on total energy calculations with no further exploration of the actual PES shape. This leaves the question open about the ground state geometry and low-temperature behavior of the E center in silicon and of the capacity of computational modelling to reproduce experimental findings.[7,8]

In the present work, by means of state-of-the-art Density Functional Theory (DFT)-based methods, we obtain the ground state geometry for different charge states, in line with the observations of Watkins *et al.*[7–9] The presence of Jahn–Teller distortions is further confirmed by accurately describing and analyzing the electronic structure of vacancy–dopant complexes by means of the many-body perturbation theory within the GW approximation. The PES shape is explored by single-point total energy calculations on interpolated geometries and by using the Climbing Image Nudged Elastic Band (CI-NEB).[17] Within this approach, we are able to reproduce the model proposed by Watkins *et al.*: three pairing degenerate minima and three resonant degenerate saddle points, with the higher energy maximum breathing mode lying at the top of the *Mexican hat* potential [see Fig. 1(b)].

Finally, by using the CI-NEB algorithm, we found energy barriers for the reorientation of the whole vacancy–dopant complex in very good agreement with the experimental measurements. For the exchange mechanism, for which no direct experimental measure is available, our results suggest a rethinking of this diffusion mechanism: the barrier, higher than what was previously postulated,[7,8] seems to indicate a relevant vacancy-mediated contribution only for the case of Sb. However, in contrast to Ref. 18, we still find the presence of a positive, if small, barrier.

II. COMPUTATIONAL DETAILS

Structural properties are obtained by means of the Density Functional Theory (DFT) as implemented in the ABINIT code.[19]

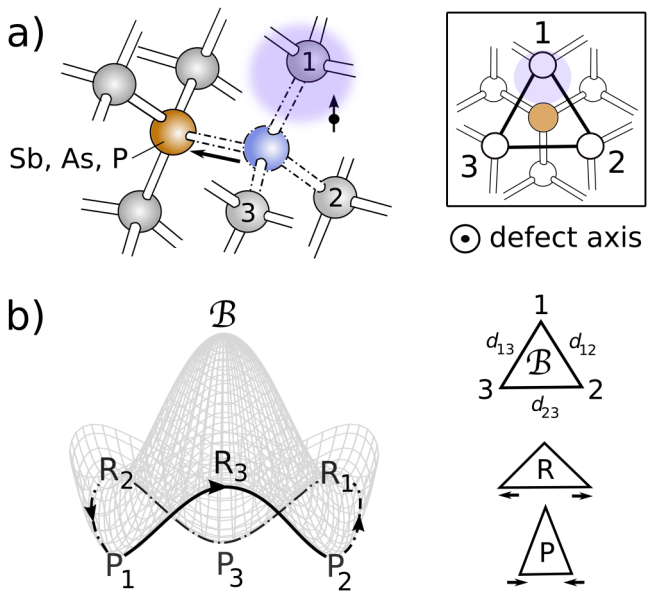

FIG. 1. The silicon E center: its projection along the vacancy–dopant axis (a) and the model of Watkins *et al.* for its potential energy surface at the neutral charge state (b). Three geometries for the E center are distinguished depending on the relative interatomic distances between atoms 1, 2, and 3: the symmetric breathing configuration ($\mathcal{B}$), the pairing configuration (P), and the resonant-bond configuration (R). P_i and R_i denote the pairing and resonant geometries with unpaired distances $d_{jk} < d_{ij} = d_{ik}$ and $d_{jk} > d_{ij} = d_{ik}$, respectively.

All reported results are based on the 216/215 atom supercell. The Brillouin zone is sampled at gamma. The ONCVPSP norm-conserving pseudopotential[20] and the Perdew–Burke–Ernserhof exchange–correlation functional[21] have been chosen. An energy cutoff for the plane-wave basis set of 762, 1306, and 1225 eV has been employed for the PV, AsV, and SbV centers, respectively, resulting in a total energy convergence below 0.5 meV, for the complexes embedded in silicon bulk. Defect geometries at different charge states have been optimized by means of the Broyden-Fletcher-Goldfarb-Shanno (BFGS) algorithm, with a convergence threshold of 1 meV/Å. All geometries discussed in the present paper were obtained without any symmetry constraint. ABINIT, as all plane-wave codes, includes a compensating background charge for all charged systems. In addition, we also turned on Makov–Payne corrections.[22]

Real space electronic densities obtained by means of DFT are plotted using the XCrySDen package.[23]

The PES is explored by both the climbing-NEB method[17] as implemented in ABINIT, with a mean total energy convergence threshold of 1 meV, and by single-point total energy calculations.

Many-body corrections are computed on top of the Kohn–Sham energies within the GW method (G_0W_0 as implemented in the ABINIT code[19,24]) in order to obtain the defect band structure correctly. We employ the Godby–Needs plasmon-pole model and a cutoff energy of 82 eV to describe the dielectric matrix. In order to assure convergence of the GW exchange–correlation self-energy, we use a very large ratio of 10:1 empty bands vs occupied bands.

Spin-unrestricted calculations are performed for the neutral charge state.

III. GROUND STATE ELECTRONIC STRUCTURE: CONFIRMATION OF THE JAHN–TELLER MODEL

The geometry of the point defect at different charge states is characterized by the interatomic distances between atoms 1, 2, and 3 in Fig. 1 (or the vacancy's first silicon neighbors). We report a pairing configuration (P in Fig. 1) as the ground state for the PV^0, AsV^0, and SbV^0 centers and a resonant geometry (R) for the negative charge states, in agreement with the experimental evidence.[7–9] The breathing mode configuration ($\mathcal{B}$ in Fig. 1) is the ground state for the three centers at a positive charge state (or an empty trap), in agreement with the previous hypothesis.[10] The characteristic interatomic distance, d_{ij}, for PV^+, AsV^+, and SbV^+ is equal to 3.54 Å, 3.59 Å, and 3.63 Å, respectively. The increase in the interatomic distance with the dopant atomic number is due to the subtle relaxation of the dopant toward the vacant site, going from its ideal substitutional site to a slight interstitial position. The dopant net displacement at a positive charge state is equal to 0.06 Å, 0.22 Å, and 0.43 Å, in ascending order of the dopant atomic number. Such a tendency is observed for all charge states, with a lower absolute displacement for 0 and −1 cases due to the increase in the electronic density at the vacant site. Such behavior is not visible by EPR spectroscopy; it does, however, have an important implication on the impurity diffusion mechanism, as discussed in Secs. V–VI.

The change in the structural configuration or Jahn–Teller distortion with the charge state can be explained through the electronic occupation of the trap-induced levels. By means of a simple one-electron molecular orbital (MO) model, the electronic configuration of the E center was described[10] as a linear combination of the three dangling bonds a_1, a_2, and a_3, located in atoms 1, 2, and 3, respectively. In the case of the breathing mode configuration, i.e., before the Jahn–Teller distortions, the lowest electronic level corresponds to the high symmetric state $S = (a_1 + a_2 + a_3)/\sqrt{3}$, whereas states $A = (2a_1 - a_2 - a_3)/\sqrt{6}$ and $B = (a_2 - a_3)/\sqrt{2}$ are higher and degenerated in energy [see Fig. 2(a)]. If the empty trap gets occupied by one or two electrons, the system undergoes a structural reconfiguration in the form of a Jahn–Teller distortion, breaking the degeneracy of states A and B. The state A is favored by the pairing configuration, P, ($\epsilon_A < \epsilon_B$), whereas the state B is lower in energy in the case of the resonant, R, configuration. A simple MO model is able to predict, for example, that at a neutral charge state, the unpaired electron is mainly located at one of the silicon neighboring atoms [atom 1 in Fig. 2(a)], as described by state A and observed by EPR spectroscopy.[7,8] It is, however, limited to the description of localized levels, overlooking the presence of bulk delocalized states, and to the use of empirical parameters when estimating the relative position of the trap levels. The splitting of the defect levels A and B after the spontaneous distortion was confirmed by optical absorption experiments[9] on the AsV^- center, where two absorption bands were reported at 0.74 eV and 1.05 eV. They were assigned to electronic excitations from an occupied localized state (S and B levels in Fig. 2) to the unoccupied state A. Unfortunately, no values for the other two dopants were reported. However, Watkins speculated that their defect-induced

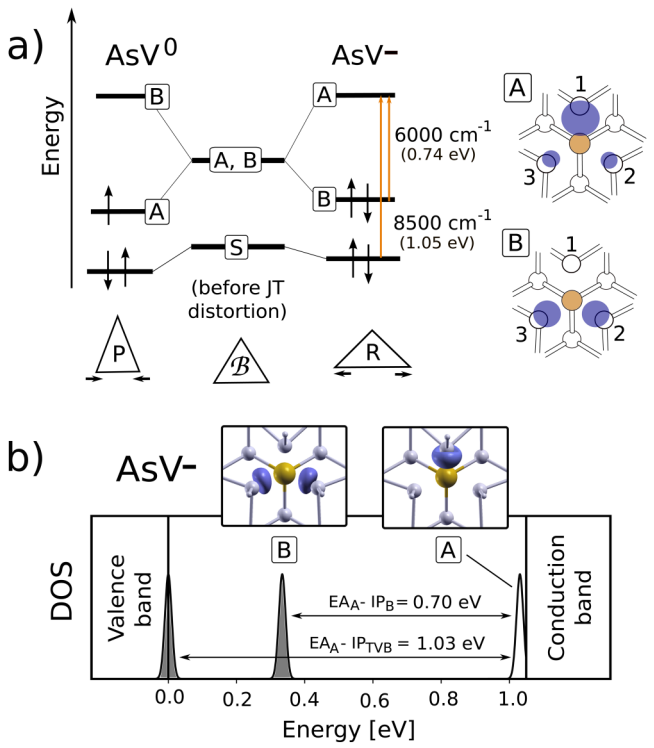

FIG. 2. Watkins's single-electron molecular orbital model[8,10] (no crystal field effects included), before and after Jahn–Teller (JT) distortions, measured optical bands,[9] and their corresponding electronic-transition assignments within Watkins's model for AsV^- (a). Computed GW density of states for AsV at a negative charge state is plotted in (b). Calculated optical absorption bands (EA_A-IP_B and EA_A-IP_{TVB}) for the AsV^- center[9] and their assignment to single-particle electronic transitions. In addition, the electronic density of the DFT-corresponding A and B states is also shown. DFT-corresponding Watkins's S state is strongly hybridized with the valence states.

optical bands should be very similar to AsV^-. Even though the electronic structure of the E center is a clear evidence of the Jahn–Teller effect, no quantitative description has so far been given due to the limitations of previously used mean-field approaches.[11–16]

Our DFT calculations qualitatively reproduce the point defect electronic structure obtained by means of simple symmetry arguments, i.e., the degeneracy of levels A and B in the absence of Jahn–Teller distortions and the splitting and reversion of such levels for the pairing and resonant configurations. Moreover, the electronic density distributions of the Kohn–Sham states A and B are in good agreement with the simple MO model (see Fig. 2). The inclusion of crystal field effects, in contrast with Watkins's simple MO model, allows us to determine that the highly symmetric S state does not appear as a disentangled localized state, but it hybridizes with the silicon bulk states, becoming part of the valence band for all charge states [and it is, therefore, not represented in Fig. 2(b)]. Defect-induced levels A and B are always found to be within the forbidden silicon band. On the other hand, the electronic state coming from the donor atom is completely

TABLE I. First excitation energies within the many-body perturbation theory in the form of the GW approximation for the E center at charge states 0 and ± 1. A and B stand for the localized defect states, whereas TVB stands for the top of the valence band.

		Center					
Charge state		PV		AsV		SbV	
+1	$EA_{A,B} - IP_{TVB}$	0.59	…	0.60	…	0.49	…
0	$EA_B - IP_A$	0.66	…	0.62	…	0.56	…
	$EA_B - IP_{TVB}$	0.88	…	0.85	…	0.75	…
−1	$EA_A - IP_B$	0.72	0.76[a]	0.70	0.74[a]	0.60	0.68[a]
	$EA_A - IP_{TVB}$	1.04	…	1.03	1.05[a]	0.89	…

[a]Measured absorption bands.[9]

disentangled from both bulk states and localized trap states S, A, and B; it is located deep in the valence band, at approximately 0.5 eV from the top of the valence band. In order to provide a quantitative description of the band structure, many-body perturbation corrections in the GW approximation[25,26] are computed on top of the DFT eigenvalues. In Fig. 2(b), we show the quasi-particle Density Of States (DOS) for the E center embedded in silicon. The semiconductor bandgap (defined as the difference between the first electronic affinity and the first ionization potential of the bulk, i.e., the bottom of the conduction band and the top of the valence band, $EA_{BCB} - IP_{TVB}$) is in agreement with the experimental value of 1.17 eV.

As the electron–hole interaction is small, because of the high macroscopic dielectric constant of silicon ($\epsilon_\infty \sim 12.0$), quasi-particle energy differences between empty and occupied states (ionization potentials and electronic affinities) can be exploited to meaningfully estimate vacancy–dopant-complex-related optical absorption bands. In the case of the AsV^- center, see Fig. 2, the energy difference between the first ionization potential (IP_B) and the first electronic affinity (EA_A) can be assigned to the 6000 cm^{-1} (0.74 eV) absorption peak reported in Ref. 9, confirming that such a transition occurs from the occupied defect state B to the unoccupied localized state A. In the case of the 8500 cm^{-1} (1.05 eV) band, we assign the measured absorption band to an electronic excitation involving the top of the valence band and the localized level A (here described as $EA_A - IP_{TVB}$). We remark that the previous assignment made by Watkins was limited to a MO model, and therefore, the position of the top of the valence band was neglected from the electronic structure prediction (see Fig. 2).

We estimate the absorption bands for PV^- and SbV^- to be located at 0.72 eV and 1.04 eV and 0.60 eV and 0.89 eV, respectively (see Table I), confirming that the E center has similar electronic properties independently of the dopant, as postulated in Ref. 9. The predicted optical absorption bands at charges states 0 and +1 are also given in Table I.

IV. LOW TEMPERATURE REGIME: THE *MEXICAN HAT* ENERGY SURFACE

We now focus our attention on the energy landscape of the E center at low temperatures, studied by EPR stress studies[7,8] in the case of the neutral charge state. As hypothesized by Refs. 7 and 8, we found three pairing configurations, P_1, P_2, and P_3 in Fig. 3(a), as ground state minima of the potential energy surface (P_i is characterized by an unpaired distance $d_{jk} < d_{ij} = d_{ik}$). The unpaired electron is, therefore, mainly located in the silicon atom i at the pairing configuration P_i (see the form of the localized state A in Fig. 2).

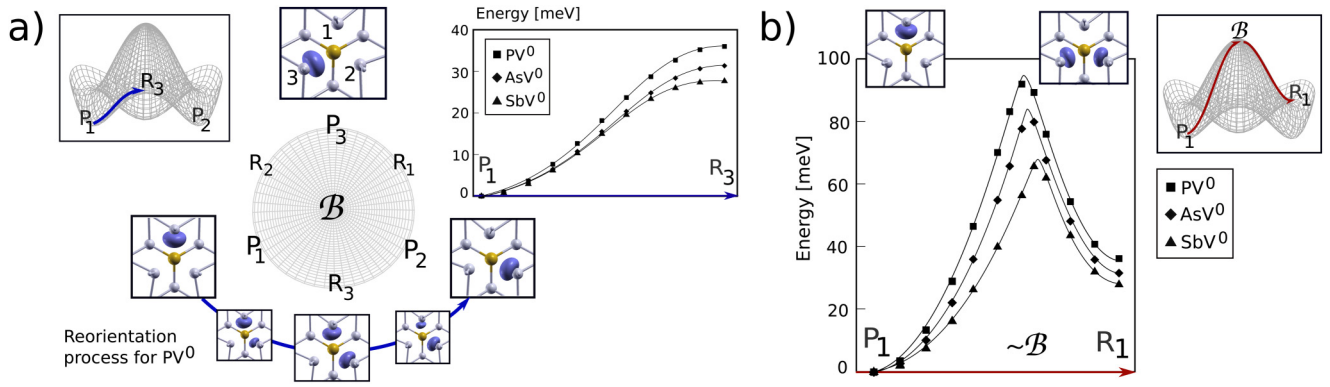

FIG. 3. Transition mechanism between pairing configurations, P, (a) and the potential energy surface (b) of E centers at a neutral charge state. The electronic density for the unpaired electron at different atomic configurations is also shown. Points are obtained within the CI-NEB algorithm (a) and single-point DFT calculations (b). Lines are a guide for the eye.

Even though the three distortions are geometrically equivalent, the electronic jumps between atoms 1, 2, and 3 modify the magnetic moment of the center, making the transitions between pairing configurations visible through EPR spectroscopy.[7,8] The lifetime of each distortion was estimated by compressing the bulk in a given spatial direction (prioritizing one of the three orientations) and studying the recovering time of the back-reorientation. The low-temperature regime reorientation barriers were estimated to be within 60–70 meV,[7,8] and it was later postulated[10] that such energy barriers actually correspond to the energy difference between the pairing and the resonant geometries. A NEB calculation between points P_1 and P_2 finds the R_3 geometry (the resonant configuration characterized by the unpaired distance $d_{12} > d_{31} = d_{32}$) as the saddle point of the transition path, proving Watkins's hypothesis regarding the height of the energy barriers between equivalent minima. We estimate the energy difference between pairing and resonant configurations to be 36 meV, 31 meV, and 28 meV for PV^0, AsV^0, and SbV^0, respectively. As in Ref. 16 that the "disagreement" between the calculated barrier, 20 meV for the AsV^0 complex, and the measured value,[8] 70 meV, was attributed to size effects, we performed calculations on a 511 atom supercell. We obtained a very similar value of about 38 meV for all three dopants, showing that size effects are particularly important for the SbV complex.

The potential energy surface for the E center at a neutral charge state is, therefore, characterized by three pairing geometries as degenerated minima, separated by three resonant configurations as saddle points [see Fig. 3(a)]. Along the Minimal Energy Path (MEP), despite structural changes between pairing and resonant configurations seem "negligible," the unpaired electron localizes at different atomic sites [see the electronic density plots that follow the symbolic paths $P_1 \rightarrow R_3 \rightarrow P_2$ in Fig. 3(a)]. At the saddle point, the system adopts a resonant configuration for which the half-filled electronic orbital becomes state B, as expected from a Jahn–Teller system [see Fig. 2(a)]. If we consider a set of configurations along a straight path between pairing and resonant configurations with the same characteristic unpaired distance, the system is forced to pass through a high symmetric configuration, close to the breathing mode geometry ($\mathcal{B}$ in Fig. 1), overcoming an energy barrier of ∼60–100 meV [see Fig. 3(b)]. According to the above results, the PES of the E center exhibits; therefore, the shape of a *Mexican hat*, in agreement with Watkins's ideas and measurements. At room temperature, the barriers between pairing configurations are comparable to $k_B T_{RT}$, and the neutral E center can reorient by circling around the *Mexican hat*. For the negative charged E centers, the *Mexican hat* is inverted: pairing and resonant configurations become, respectively, saddles and minima points. The energy barriers to jump from one minimum, R configuration, to another one is of 62 meV, 48 meV, and 25 meV for PV^-, AsV^-, and SbV^-, respectively (511 atom supercell) at the DFT level of approximation. As in the neutral case, size effects are important when computing such a reorientation barrier, resulting in up to a 20 meV energy difference between 215 and 511 silicon supercells. Positively charged E centers exhibit a single minimum that corresponds to the breathing configuration, $\mathcal{B}$.

The systematic underestimation of the barriers, 40 meV for all three dopants, against the 60–70 meV measured by Watkins *et al.*,[7,8] is a signature of the well known self-interaction problem in standard DFT exchange and correlation functionals. A combined DFT-GW approach, as previously exploited to correct total energy differences in point-defect studies,[27,28] is here used to correct barriers as follows. By definition, the ionization potential computed within the GW method for the pairing configuration ($\mathbf{R}_P$) at a neutral charge state can be written as a total energy difference, IP ($\mathbf{R}_P$, 0) = E ($\mathbf{R}_P$, 0) − E ($\mathbf{R}_P$, +). By computing the same quantity at the resonant configuration, the reorientation barrier at a neutral charge state can be written as ΔE ($\mathbf{R}_P$,$\mathbf{R}_R$; 0) = IP ($\mathbf{R}_P$, 0) − ΔE ($\mathbf{R}_P$,$\mathbf{R}_R$; +) − IP ($\mathbf{R}_R$, 0). The quantity ΔE ($\mathbf{R}_P$,$\mathbf{R}_R$; +) is the difference in the energy between the pairing and resonant configurations at a positive charge state (empty trap) and, therefore, can be safely estimated within DFT. In the case of the PV center (where the elastic contributions are minimal at 216 atoms), such a difference in ionization potentials, IP ($\mathbf{R}_P$, 0) − IP ($\mathbf{R}_R$, 0), is equal to 65 meV, and the corresponding reconfiguration energy, ΔE ($\mathbf{R}_P$,$\mathbf{R}_R$; +), is 10 meV, given an overall reorientation barrier of 75 meV. Similarly, a value of 71 meV is obtained for the AsV center.

V. HIGH-TEMPERATURE DYNAMICS: VACANCY–DOPANT COMPLEX REORIENTATION AND EXCHANGE

The present section is dedicated to the two mechanisms underlying the vacancy-mediated dopant diffusion: the defect reorientation and the vacancy–dopant exchange [see Fig. 4(a)]. The first process involves the reorientation of the vacancy–dopant axis, through the movement of the vacancy to second [vacancy positions 2 and 2′ in Fig. 4(a)] and third neighbor positions (denoted 3) with respect to the impurity. Such a mechanism was first proposed by Refs. 7 and 8, after performing EPR stress studies at high temperatures. They obtained the lifetime of each defect-axis orientation, corresponding to activation energies that were comprised between 0.9 and 1.3 eV, for dopant-increasing atomic number. As in the case of low temperature studies, a characterization of the atomic process and its energy landscape at high temperatures is possible by EPR spectroscopy due to the change in the magnetic moment between the initial and final configurations [see configurations 1 and 1′ in Fig. 4(b)]. It was also postulated that the reorientation mechanism constituted the bottleneck process for vacancy-mediated diffusion, since the energy expense for the dopant–vacancy exchange was believed to be close to 0.33 eV (activation energy for the monovacancy diffusion in silicon[29]).

The high temperature dynamics of the E center is studied through the mechanisms of defect reorientation and dopant–vacancy exchange within the CI-NEB algorithm.[17] The exchange of positions between the dopant and vacancy is a direct symmetric process, as shown in Fig. 4(b). The decrease in the energy barrier with the increase in the dopant size is explained by the ground state geometry of the E center. As mentioned in Sec. III, the dopant slightly moves from its ideal substitutional position toward the vacant site. Such an effect increases with the dopant size, as it is evident by the low energy barrier obtained, in particular, for the antimony–vacancy exchange. In contrast with the simple exchange process, the reorientation of the defect axis requires the movement of the vacancy to different sites of the lattice before arriving to its final configuration. In order to compute the minimal energy path between equivalent positions 1 and 1′, a preliminary study of

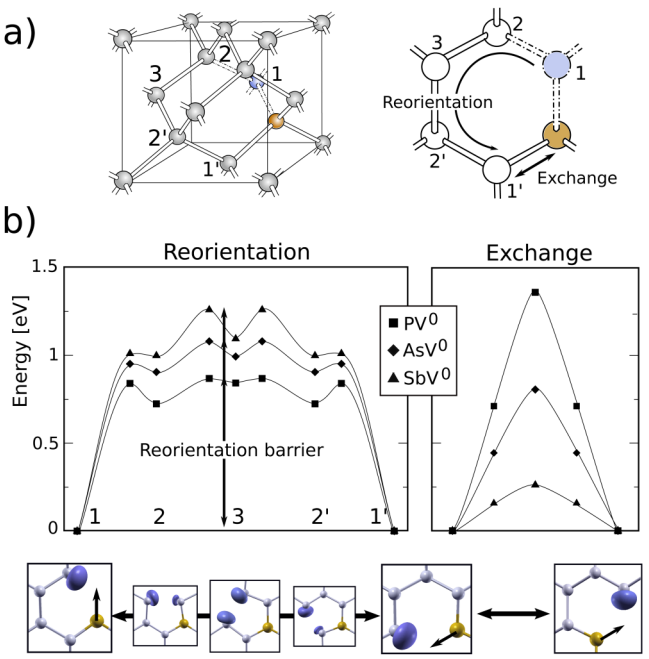

FIG. 4. The vacancy-mediated dopant diffusion mechanisms: the reorientation of the defect and the exchange vacancy–dopant (a) and their computed energy landscapes (b). The probability density for the unpaired electron along both processes is shown. Only relevant points, corresponding to the local minimum and saddle points, are shown in the case of the reorientation process. Lines are guides to the eye.

transient geometries is required. Geometry relaxation calculations were made for the vacancy at second and third neighbor positions from the dopant in order to specify the beginning and ending points of consecutive NEB calculations [see Fig. 4(b)]. Two different minimal energy paths are, therefore, characterized ($1 \rightarrow 2$ and $2 \rightarrow 3$), with their respective energy barriers. The relative stability of the second neighbor and third neighbor configurations presents opposite tendencies with the dopant size. The E center is barely stable at the third neighbor configuration in the case of the PV^0 center, finding an energy barrier of 26 meV, whereas the energy expense to leave such a configuration is about 0.16 eV in the case of the antimony. As shown in Fig. 4(b), such behavior is inverted in the case of the second neighbor configuration, obtaining energy barriers to return to the first neighbor site of 11 meV for SbV^0 and 0.11 eV for PV^0. The reorientation barrier observed by EPR stress studies at high temperatures[7,8] is here estimated as the energy difference between the ground state configuration of the E center and the saddle point of the $2 \rightarrow 3$ transition (see Fig. 4).

The theoretical values obtained in Table II clearly show that the diffusion of the whole vacancy–dopant complex is energetically more expensive in the case of the PV center than postulated by Ref. 7 from the mono-vacancy diffusion.[29] While a detailed study of the diffusion mechanism of the E center is beyond the scope of the present work, our results indicate that vacancy-mediated diffusion would be the primary diffusion mechanism for large dopant atomic numbers, as it has been experimentally proved in Ref. 6.

TABLE II. Exchange barriers, first neighbor binding energies, and reorientation barriers at high temperatures for PV^0, AsV^0, and SbV^0. Values are given in eV. TW stands for this work, whereas OW stands for other works.

	Exchange barrier		1st neighb. binding energy		Reorientation barrier		
Dopant	TW	OW	TW	OW	TW	OW	Exp.
P	1.36	1.05,[18] 1.29[30]	0.84	1.05[18]	0.87	0.8[30]	0.93[7]
As	0.81	0.65[18]	0.95	1.17[18]	1.07	1.0[16]	1.07[8]
Sb	0.26	−0.05[18]	1.01	1.45[18]	1.26	…	1.28[8]

VI. CONCLUSIONS

In conclusion, we provide a comprehensive theoretical picture of the silicon E center comprising structural, electronic, and optical properties, together with their low- and high-temperature behavior, which ultimately complies with experiments.

The electronic ground state of the silicon E center is explained through a symmetry-based Jahn–Teller model: the trap-induced states can recombine to lower the defect energy by distorting the symmetric breathing geometry into a pairing configuration (at a neutral charge state) or a resonant configuration (a negative charge state). The relative position of these localized states (states A and B in Fig. 2) can be accurately reproduced by many-body perturbation calculations within the GW approximation. The calculated defect-related optical absorption bands are located at 0.70 eV and 1.03 eV for the AsV^- complex and at 0.72 eV and 0.60 eV for the PV^- and SbV^- centers, in very good agreement with the measured bands at 0.74, 1.05, 0.76, and 0.68 eV, respectively. First-principles studies beyond the DFT method confirm that the E center presents similar optical and electronic properties independently of the dopant.

Thanks to an exhaustive first-principles exploration of the E center PES, we confirm that it exhibits the shape of a *Mexican hat*, in agreement with the measurements of Watkins *et al.* We find three degenerate pairing configurations (P in Fig. 1) as a ground state for PV^0, AsV^0, and SbV^0 separated by three resonant (R in Fig. 2) configurations as saddle points. Such centers are, therefore, not *metastable* as was reported and/or inferred in previous theoretical calculations.[14,15] At a negative charge state, the resonant configuration becomes the minima of the *sombrero*, while the pairing configurations become unstable. The energy barriers encountered at low temperatures between *equivalent* minima are correctly estimated only when the electronic interaction is treated *accurately* within the GW approximation.

At higher temperatures, we explore the energy landscape for the vacancy–dopant axis reorientation, finding activation energy barriers in very good agreement with experiments. Moreover, the computed exchange barriers offer new insight on the vacancy-mediated diffusion. In particular, in the case of the SbV complex,

they support the long time belief that Sb diffuses in silicon mainly through a vacancy-mediated mechanism.

REFERENCES

[1]P. Pichler, *Intrinsic Point Defects, Impurities, and Their Diffusion in Silicon* (Springer Science & Business Media, 2012), Chap. 5.
[2]I. H. Hopkins and G. R. Hopkinson, "Further measurements of random telegraph signals in proton irradiated CCDs," IEEE Trans. Nucl. Sci. **42**, 2074–2081 (1995).
[3]D. Smith, A. Holland, and I. Hutchinson, "Random telegraph signals in charge coupled devices," Nucl. Instrum. Methods Phys. Res. A **530**, 521–535 (2004).
[4]T. Nuns, G. Quadri, J. David, and O. Gilard, "Annealing of proton-induced random telegraph signal in CCDs," IEEE Trans. Nucl. Sci. **54**, 1120–1128 (2007).
[5]C. Virmontois, V. Goiffon, P. Magnan, O. Saint-Pe, S. Girard, S. Petit, G. Rolland, and A. Bardoux, "Total ionizing dose versus displacement damage dose induced dark current random telegraph signals in cmos image sensors," IEEE Trans. Nucl. Sci. **58**, 3085–3094 (2011).
[6]A. Ural, P. B. Griffin, and J. D. Plummer, "Fractional contributions of microscopic diffusion mechanisms for common dopants and self-diffusion in silicon," J. Appl. Phys. **85**, 6440–6446 (1999).
[7]G. D. Watkins and J. W. Corbett, "Defects in irradiated silicon: Electron paramagnetic resonance and electron-nuclear double resonance of the Si-E center," Phys. Rev. **134**, A1359–A1377 (1964).
[8]E. L. Elkin and G. D. Watkins, "Defects in irradiated silicon: Electron paramagnetic resonance and electron-nuclear double resonance of the arsenic- and antimony-vacancy pairs," Phys. Rev. **174**, 881–897 (1968).
[9]G. D. Watkins, "Optical properties of group-V atom-vacancy pairs in silicon," Radiat. Eff. Defects Solids **111-112**, 487–500 (1989).
[10]G. Watkins, "Understanding the Jahn–Teller distortions for the divacancy and the vacancy–group-V-atom pair in silicon," Phys. B: Condens. Matter **376-377**, 50–53 (2006).
[11]R. Virkkunen and R. Nieminen, "First-principles study of the phosphorous-vacancy pair in silicon," Comput. Mater. Sci. **1**, 351–357 (1993).
[12]G. Pfanner, C. Freysoldt, J. Neugebauer, and U. Gerstmann, "Ab initio EPR parameters for dangling-bond defect complexes in silicon: Effect of jahn-teller distortion," Phys. Rev. B **85**, 195202 (2012).
[13]M. G. Ganchenkova, A. Y. Kuznetsov, and R. M. Nieminen, "Electronic structure of the phosphorus-vacancy complex in silicon: A resonant-bond model," Phys. Rev. B **70**, 115204 (2004).
[14]A. N. Larsen, A. Mesli, K. Bonde Nielsen, H. K. Nielsen, L. Dobaczewski, J. Adey, R. Jones, D. W. Palmer, P. R. Briddon, and S. Öberg, "*e* center in silicon has a donor level in the band gap," Phys. Rev. Lett. **97**, 106402 (2006).
[15]M. Ganchenkova, L. Oikkonen, V. Borodin, S. Nicolaysen, and R. Nieminen, "Vacancies and E-centers in silicon as multi-symmetry defects," Mater. Sci. Eng. B **159–160**, 107–111 (2009). eMRS 2008 Spring Conference Symposium K: Advanced Silicon Materials Research for Electronic and Photovoltaic Applications.
[16]S. Öğüt and J. R. Chelikowsky, "Charge state dependent Jahn-Teller distortions of the E-center defect in crystalline Si," Phys. Rev. Lett. **91**, 235503 (2003).
[17]G. Henkelman, B. P. Uberuaga, and H. Jónsson, "A climbing image nudged elastic band method for finding saddle points and minimum energy paths," J. Chem. Phys. **113**, 9901–9904 (2000).
[18]J. S. Nelson, P. A. Schultz, and A. F. Wright, "Valence and atomic size dependent exchange barriers in vacancy-mediated dopant diffusion," Appl. Phys. Lett. **73**, 247–249 (1998).
[19]X. Gonze, F. Jollet, F. Abreu Araujo, D. Adams, B. Amadon, T. Applencourt, C. Audouze, J.-M. Beuken, J. Bieder, A. Bokhanchuk, E. Bousquet, F. Bruneval, D. Caliste, M. Côté, F. Dahm, F. Da Pieve, M. Delaveau, M. Di Gennaro, B. Dorado, C. Espejo, G. Geneste, L. Genovese, A. Gerossier, M. Giantomassi, Y. Gillet, D. Hamann, L. He, G. Jomard, J. Laflamme Janssen, S. Le Roux, A. Levitt, A. Lherbier, F. Liu, I. Lukačević, A. Martin, C. Martins, M. Oliveira, S. Poncé, Y. Pouillon, T. Rangel, G.-M. Rignanese, A. Romero, B. Rousseau, O. Rubel, A. Shukri, M. Stankovski, M. Torrent, M. Van Setten, B. Van Troeye, M. Verstraete, D. Waroquiers, J. Wiktor, B. Xu, A. Zhou, and J. Zwanziger, "Recent developments in the ABINIT software package," Comput. Phys. Commun. **205**, 106–131 (2016).
[20]D. R. Hamann, "Optimized norm-conserving Vanderbilt pseudopotentials," Phys. Rev. B **88**, 085117 (2013).
[21]J. P. Perdew, K. Burke, and M. Ernzerhof, "Generalized gradient approximation made simple," Phys. Rev. Lett. **77**, 3865–3868 (1996).
[22]G. Makov and M. C. Payne, "Periodic boundary conditions in *ab initio* calculations," Phys. Rev. B **51**, 4014–4022 (1995).
[23]A. Kokalj, "XCrySDen–a new program for displaying crystalline structures and electron densities," J. Mol. Graph. Model. **17**, 176–179 (1999).
[24]F. Bruneval, N. Vast, and L. Reining, "Effect of self-consistency on quasiparticles in solids," Phys. Rev. B **74**, 045102 (2006).
[25]L. Hedin, "New method for calculating the one-particle Green's function with application to the electron-gas problem," Phys. Rev. **139**, A796–A823 (1965).
[26]L. Hedin and S. Lundqvist, *Effects of Electron-Electron and Electron-Phonon Interactions on the One-Electron States of Solids* (Academic Press, 1970), pp. 1–181.
[27]P. Rinke, A. Janotti, M. Scheffler, and C. G. Van de Walle, "Defect formation energies without the band-gap problem: Combining density-functional theory and the GW approach for the silicon self-interstitial," Phys. Rev. Lett. **102**, 026402 (2009).
[28]L. Martin-Samos, G. Roma, P. Rinke, and Y. Limoge, "Charged oxygen defects in SiO_2: Going beyond local and semilocal approximations to density functional theory," Phys. Rev. Lett. **104**, 075502 (2010).
[29]G. Watkins, "An EPR study of the lattice vacancy in silicon," J. Phys. Soc. Jpn. **18**(Suppl. II), 22 (1963).
[30]X.-Y. Liu, W. Windl, K. M. Beardmore, and M. P. Masquelier, "First-principles study of phosphorus diffusion in silicon: Interstitial- and vacancy-mediated diffusion mechanisms," Appl. Phys. Lett. **82**, 1839–1841 (2003).